Published in final edited form as:
J Neurooncol. 2011 November ; 105(2): 241–251. doi:10.1007/s11060-011-0604-7.

Vorinostat modulates cell cycle regulatory proteins in glioma cells and human glioma slice cultures

Jihong Xu,
Department of Neuro-Oncology, The Brain Tumor Center, University of Texas M. D. Anderson Cancer Center, 1515 Holcombe Blvd., Unit 431, Houston, TX 77030, USA

Deepa Sampath,
Department of Experimental Therapeutics, University of Texas, M. D. Anderson Cancer Center, Houston, TX, USA

Frederick F. Lang,
Department of Neurosurgery, The Brain Tumor Center, University of Texas M. D. Anderson Cancer Center, Houston, TX, USA

Sujit Prabhu,
Department of Neurosurgery, The Brain Tumor Center, University of Texas M. D. Anderson Cancer Center, Houston, TX, USA

Ganesh Rao,
Department of Neurosurgery, The Brain Tumor Center, University of Texas M. D. Anderson Cancer Center, Houston, TX, USA

Gregory N. Fuller,
Department of Neuropathology, The Brain Tumor Center, University of Texas M. D. Anderson Cancer Center, Houston, TX, USA

Yuanfang Liu, and
Department of Neuro-Oncology, The Brain Tumor Center, University of Texas M. D. Anderson Cancer Center, 1515 Holcombe Blvd., Unit 431, Houston, TX 77030, USA

Vinay K. Puduvalli
Department of Neuro-Oncology, The Brain Tumor Center, University of Texas M. D. Anderson Cancer Center, 1515 Holcombe Blvd., Unit 431, Houston, TX 77030, USA
vpuduval@mdanderson.org

Abstract

Chromatin modification through histone deacetylase inhibition has shown evidence of activity against malignancies. The mechanism of action of such agents are pleiotropic and potentially tumor specific. In this study, we studied the mechanisms of vorinostat-induced cellular effects in gliomas. The effects of vorinostat on proliferation, induction of apoptosis and cell cycle effects were studied in vitro (D54, U87 and U373 glioma cell lines). To gain additional insights into its effects on human gliomas, vorinostat-induced changes were examined ex vivo using a novel organotypic human glioma slice model. Vorinostat treatment resulted in increased p21 levels in all glioma cells tested in a p53 independent manner. In addition, cyclin B1 levels were transcriptionally downregulated and resulted in reduced kinase activity of the cyclin B1/cdkl

Correspondence to: Vinay K. Puduvalli.

Conflict of interest The authors declare no conflicts of interest related to this study.

complex causing a G2 arrest. These effects were associated with a dose- and time-dependent inhibition of cellular proliferation and anchorage-independent growth in association with hyperacetylation of core histones and induction of apoptosis. Of particular significance, we demonstrate histone hyperacetylation and increased p21 levels in freshly resected human glioma specimens maintained as organotypic slice cultures and exposed to vorinostat similar to cell lines suggesting that human glioma can be targeted by this agent. Our data suggest that the effects of vorinostat are associated with modulation of cell cycle related proteins and activation of a G2 checkpoint along with induction of apoptosis. These effects are mediated by both transcriptional and post-translational mechanisms which provide potential options that can be exploited to develop new therapeutic approaches against gliomas.

Keywords

Histone deacetylase inhibitors; Malignant glioma; Apoptosis; Cell cycle arrest; Organotypic slice cultures

Introduction

Genetic alterations are known to be critical to tumorigenesis and progression in malignant gliomas [1,2]. However, epigenetic mechanisms play an equally important role in tumorigenesis and response to therapeutic agents [3, 4]. Promoter methylation, which affects expression of genes such as *MGMT* (*O*–6 methyl guanine methyl transferase), is a recognized epigenetic mechanism associated with gene silencing in primary brain tumors [5–8]. However, other epigenetic alterations including changes in chromatin structure by histone modification and regulatory effects of microRNA can alter gene expression and dramatically influence growth, viability and response to therapy of malignant cells. Of such epigenetic alterations, modifications of the core nucleosomal histones, H3 and H4, including by phosphorylation, methylation or acetylation is especially relevant. In particular, acetylation of core histones by histone acetyl transferases (HAT) (which results in an open chromatin configuration associated with gene expression) and or their deacetylation by histone deacetylases (HDAC) (which causes compaction of chromatin and silencing of gene expression) are dynamically balanced processes which can become imbalanced in malignancies resulting in overactivity of HDACs.

Novel agents that target epigenetic processes in malignancies have been recently developed; HDAC inhibitors are one such class of agents which have demonstrated potential for in vitro and in vivo activity against malignant cells [9] and are being assessed as a therapeutic strategy against malignancies. Preclinical studies have shown that HDAC inhibitors such as trichostatin A and butyrates can inhibit proliferation and induce apoptosis of glioma cells [10, 11], but are unsuitable for human studies due to toxicity. Of the recently developed HDAC inhibitors, vorinostat (suberoylanilide hydroxamic acid, SAHA) has shown in vitro and in vivo activity against several malignancies [9, 12–15]. Vorinostat is well tolerated by humans, is readily bioavailable upon oral administration and crosses the intact blood brain barrier [16, 17]. Based on its activity against cutaneous T-cell lymphoma, it received regulatory approval for clinical use against this disease [13]. In this study, we examined the mechanisms by which vorinostat exerts its effects upon proliferation of glioma cells and assessed its effects on cultured viable human glioma slices to validate the signaling pathways relevant to its activity against this malignancy. We demonstrate that vorinostat increases p21 levels and transcriptionally down regulates cyclin B1 which is associated with a G2 phase cell cycle arrest and apoptosis in glioma cells; we also demonstrate that similar changes are evident in human glioma tissue in slice culture indicating that vorinostat will likely induce antitumor effects in humans.

Materials and methods

Cell lines and drug

Cell lines were derived from human malignant gliomas and were maintained in DMEM-F12 (1:1, v/v) medium (Sigma Chemical Co., cat # 5144-5C) supplemented with 5% fetal calf serum, at 37°C in a humidified atmosphere containing 5% CO_2. D54MG cells were kindly provided by Dr. Darrell Bigner (Duke University, Durham, NC) and U251HF, by Dr Sandra A. Rempel (Henry Ford Hospital, Detroit, MI). U373 and U87MG cells were purchased from American Tissue Type Collection (ATCC). Normal human astrocytes (NHA) (Lonza Inc, Clonetics C-2665) were maintained in Astrocyte Basal medium (Lonza Inc, CC-3186) and cultured according to manufacturer's instructions. Vorinostat was kindly provided by Aton Pharma (now Merck & Company, New Jersey, NJ). Glioma cell lines were authenticated by short tandem repeat DNA fingerprinting in the brain tumor center core facility.

WST-1 assay

Cell proliferation and viability of glioma cells were determined using the colorimetric WST-1 assay (Roche Applied Sciences, Indianapolis, IN) according to the manufacturer's specifications. Briefly, 3×10^3 cells/well were plated in triplicate in 96-well cell culture plates and the cells were exposed to vorinostat at increasing concentrations for the period. The WST reagent at a 10% dilution was added to each well for 1 h and the spectrophotometric absorbance was measured using an ELISA plate reader at 450 nm as a measure of the viable cell fraction.

Soft agar clonogenic assay

Cells were plated at a density of 5 × 10 cells and treated with vorinostat (3 or 5 μM) for 24 h. The treated cells were subsequently replated in six well plates along with untreated control cells in triplicate at a density of 200–500 cells per well (depending on the cell line) to get a single cell distribution in 0.3% soft agar with a 0.8% agar underlay and incubated for approximately 13–20 days depending on the cell line. The plates were overlaid with 1 ml FBS-containing medium every 3–4 days. Colonies larger than 50 urn in size were counted and the number of colonies in 15 contiguous fields (5× magnification) was counted in three independent experiments; the average number of colonies per field was calculated and represented graphically.

Cell synchronization

To synchronize cells in G1/S boundary, exponentially growing glioma cells were exposed 24 h after plating to 2 mM thymidine (Sigma-Aldrich, cat # T1895) for 18 h. The thymidine-containing medium was then removed and normal growth medium was added. After 6×8 h, 1.2 mM hydroxyurea was added for an additional 16 h. Cells were then released from the double block, treated with vorinostat 5 μM and harvested at various time points for flow cytometry analysis.

Flowcytometric analysis

Cell cycle kinetics were analyzed by flowcytometry as previously described [18].

Terminal deoxynucleotidyl transferase (TdT)-mediated dUTP nick end-labeling (TUNEL) assay

To detect DNA fragmentation generated by apoptosis and its relation to the cell cycle phase, a TUNEL assay was performed using a commercially available kit (Phoenix Flow systems, Inc. APO-Direct, AD-1001) according to manufacturer's instructions. Briefly, cells were

fixed on ice with 1% (w/v) paraformaldehyde, washed thrice with PBS and stored in 70% ice-cold ethanol until flowcytometric analysis. The cells were incubated in DNA staining solution (consisting of TdT enzyme, reaction buffer and FITC-dUTP in ddH20) with appropriate positive and negative controls and subsequently counterstained with PI/RNase solution for flowcytometric analysis. TUNEL positivity and cell cycle changes were analyzed using a laser scanning flowcytometer (Beckton Dickinson) equipped with a 488 nm Argon Laser. The use of a dual parameter display method permitted both the detection of TUNEL positive cells and resolution of the cell cycle phase that they emerged from.

Western blot analysis and antibodies

Changes in protein expression were studied by western blot analysis in various experiments at the indicated times after exposure to drug as previously described [18]. Analysis was repeated at least twice to confirm the results. Briefly, 20 μg of protein sample was subjected to SDS-PAGE subsequently immunoblotted using the following antibodies: mouse anti-p21 (Calbiochem, OP64), cyclin B1 (Santa Cruz Biotechnology), acetyl histone H3 (06–599), histone H3 (06–765) and acetyl histone H4 (06–598) (Upstate Biotech); rabbit anti-phospho-p53 (Ser-15 #9284); rabbit anti-phospho cdk1 (Tyr-15) and rabbit anti-cdc25c (Cell Signaling Technology). Horseradish peroxidase-conjugated donkey anti-rabbit and goat anti-mouse antibodies (Amer-sham Corp.) were used as secondary antibodies. Actin levels were determined as a loading control using a mouse anti-hunan β-actin monoclonal antibody (Amersham Corp.).

Quantitative real-time polymerase chain reaction (qRT-PCR)

Total RNA was extracted using the RNeasy Mini Kit (Qiagen, Cat # 75106) according to the manufacturer's instructions. For each RNA sample, a 1-μg aliquot was reverse transcribed into cDNA using the Transcriptor First Strand cDNA Synthesis Kit (Roche, Cat #: 04379012001). Real time PCR was performed using the ™SYBR Green SuperMix (Bio-Rad, Cat # 170–8884) and the DNA Engine Chromo4 System (MJ Research, Waltham). The following primer pairs were utilized: p21 sense (180–199) AGCTGA GCCGCGACTGTGAT, anti-sense (464–145) CTGAGCG AGGCACAAGGGTA; Cyclin B1 sense (348–367) GGCC AAAATGCCTATGAAGA, anti-sense (576–557) AGAT GTTTCCATTGGGCTTG. Data analysis was performed using the Opticon Monitor™ Software.

Organotypic human glioma slice cultures

Tissue from resections of recurrent malignant gliomas was obtained under an institutional review board approved protocol with the written informed consent of the patients undergoing surgery. Patients were informed about the nature of the experiments related to ex vivo slice cultures and offered the opportunity to participate by consenting to provide residual tissue obtained from surgery for this study including nontumor tissue. The tissue specimen was rapidly transported to the laboratory on ice, transferred into ice cold carbogenated cutting solution (110 mM sucrose, 60 mM NaCl, 3 mM KC1, 1.25 mM NaH_2PO_4, 28 mM $NaHCO_3$, 0.5 mM, $CaCl_2$, 5 mM D-glucose, and 0.6 mM ascorbate); living glioma slices (300 μM thick) were generated using a vibrating microtome (Vibratome 1500 series, Vibratome, St. Louis, MO) and transferred to ice cold artificial cerebrospinal fluid (ACSF: 125 mM NaCl, 2.5 mM KCl, 1.24 mM, NaH_2PO_4, 25 mM $NaHCO_3$, 10 mM D-glucose, 2 mM $CaCl_2$, and 1 mM $MgCl_2$). The slices were then equilibrated in ACSF at room temperature for 30 min and subsequently transferred to tissue culture dishes (3–4 slices per condition) containing DMEM-F12 with fetal bovine serum/antibiotic and incubated at 37°C. To determine viability of the slices, the freshly obtained slices were transduced 2 h after plating with an adenoviral construct which expresses enhanced green fluorescent protein (Ad-EGFP) and EGFP expression monitored by fluorescent microscopy.

Standardization experiments using over 10 consecutive slice cultures examined over 10 HPF fields for EGFP expression showed that well selected slices from solid tumor tissue without areas of necrosis retain over 80% viability over a period of 7 to 21 days. In our experiments, we utilized 3–5 slices per condition (0.5 cm × 0.5 cm × 300 μm) which on the average contain 2–5 × 10^5 viable cells/slice. Most experiments done in this study were done over a 48–96 h period which was within the viability period for the slices.

Drug treatment of glioma slice cultures

Tumor slices were obtained from freshly collected specimens as described above, allowed to equilibrate overnight in culture and treated with either PBS or vorinostat (3 μM) for various periods prior to harvesting. Medium was changed every 3 days without further addition of drug. Protein lysates were generated and used in western blot experiments.

Results

Vorinostat mediated induction of core histone hyperacetylation and inhibition of glioma cell proliferation

Glioma cells (D54MG, U87MG, U373, and U251HF), exposed to vorinostat and examined using a WST-1 proliferation assay, showed a dose-dependent decrease in proliferation over a 72 h period (Fig. 1a). Additionally, in a test of anchorage-independent growth in a soft agar colony-forming assay, which has been correlated with tumorigenicity in vivo, glioma cells exposed to vorinostat formed significantly fewer and smaller colonies in a dose-dependent manner compared with vehicle treated controls (Fig. 2b).

In the glioma cells exposed to vorinostat, hyperacetylation of histone H3 and H4, a direct consequence of HDAC inhibition, was seen in a dose dependent manner following addition of vorinostat both at a high (Fig. 1c) and a low dose range (Fig. 1d); in addition, a time-dependent increase in histone hyperacetylation was seen beginning as early as 15 min and remained high for over 24 h indicating a early onset and sustained effect of the drug; these changes were not as a result on increase in total histone levels (Fig. 1e).

Induction of G2 phase cell cycle arrest followed by apoptosis in response to vorinostat

HDAC inhibitors induce changes in cell cycle kinetics including a G1 or a G2/M phase arrest [19]. In glioma cells exposed to vorinostat for 24 or 48 h, a G2/M phase arrest was seen with appearance of a subG1 fraction in D54 and U373 cells, and less prominently in U87 cells (Fig. 2a). In order to better define these changes, the cells were synchronized in the G1/S boundary by a thymidine/hydroxyurea double block and released [20]. Exposure to vorinostat under these conditions demonstrated that the G2/M accumulation of cells preceded induction of apoptosis (Fig. 2b). Apoptosis was also evident by TUNEL assay by 24 h after exposure to vorinostat (data not shown). We also tested the effects of vorinostat against NHA; as with the glioma cells, NHA also demonstrated increase in p21 levels and histone hyperacetylation suggesting activation of similar signaling pathways in glioma and NHA (Fig. 2c). These findings were associated with the appearance of an apoptotic (sub-G1) fraction but there was no G2 arrest raising the possibility that the cell cycle effects of this agent are distinct from its induction of apoptosis in NHA (Fig. 2d—also see “Discussion” section).

Characterization of cell cycle arrest by vorinostat

To further characterize the nature of the G2/M arrest, semiconfluent D54MG cells were exposed to vorinostat (3 μM) 24 h after plating and harvested at 24, 48 and 72 h after treatment. The cells were stained with DAPI (to determine total cell number) and anti-phospho-histone H3 antibody (to identify mitotic cells). By immunofluorescent microscopy,

the antiproliferative effects of vorinostat were manifest as a reduction in total number of cells (Fig. 2e, upper panels) but in addition, a striking reduction of phospho histone-H3 stained (mitotic) cells was also seen (Fig. 2e, lower panels). These data when combined with the flowcytometric analysis confirms that vorinostat induces a G2 and not an M phase arrest cycle in gliomas.

Changes in p21 levels following exposure to vorinostat

In order to determine the mechanism by which the G2 checkpoint was activated, we studied the effect of vorinostat on checkpoint proteins associated with the G2/M boundary. An upregulation of p21 protein levels was seen in response to vorinostat as early as 30 min post treatment with levels remaining elevated at 24 h (Fig.3a). Dose-dependent increase in p21 was not seen beyond 5 μM suggesting a saturation of this mechanism (Fig. 3b); upregulation of p21 was seen at doses of vorinostat as low as 1 μM (Fig. 3c). To determine if p21 upregulation was a result of p53 activation, we assessed levels of Ser-15 phosphorylation of p53 (activated) in D54 and U87 cells which express wild type p53. There was no evidence of increase in phospho-p53 levels suggesting lack of activation of p53; on the contrary, a decrease in p53 levels (total and phosphorylated forms) was seen by 24 h after exposure to vorinostat (Fig. 3d). These results suggest that upregulation of p21 was mediated by a p53 independent mechanism.

Effects of vorinostat on cdk1 and cdc25c, the G2/M checkpoint regulatory proteins

The transition of cells from the G2 phase of the cell cycle to mitosis is governed by the action of cdk1, a cyclin dependent kinase, in association with cyclin B1. Cdk1 is maintained in an inactive state by phosphorylation of two residues at its ATP binding site (Thr-14 and Tyr-15). At the transition from G2 phase to mitosis, a decrease in inhibitory phosphorylation of cdc25c, a phosphatase, at the Ser-216 residue permits it to activate cdk1 by dephosphorylating it at its Thr-14 and Tyr-15 residues [21]. We examined the levels of expression of total and phosphorylated forms of these cell cycle regulatory proteins including cdk1, cdc25c and cyclin B1. Phospho-cdk1 (Tyr-15) levels decreased significantly in a dose dependent manner at 24 and 48 h after vorinostat treatment whereas total cdk1 levels decreased only slightly (Fig. 4a). Because this finding implied activation of cdk1 by changes in cdc25c, we examined the phospho and total levels of this protein. Vorinostat treated glioma cells showed an initial increase in phosphorylated form followed by a decrease in levels of both the Ser-216 phosphorylated and total cdc25c forms in a dose (Fig. 4b) and time dependent manner (Fig. 4c). We also assessed changes in levels of both total and phospho-cdk1 over a period between 15 min and 24 h of vorinostat addition (Fig. 4d). After a transient increase in total cdk1 levels beginning within 15 min of vorinostat addition, the levels decreased between 9 and 24 h in both D54 and U87 cells. Similarly, a transient increase followed by a more sustained decrease in levels of inhibitory phosphorylation of cdk1 at Tyr-15 residue was seen, a decrease in phospho-cdk1 levels was seen in glioma cells but not in NHA. The differential effects upon cdk1 and cdc25c in NHA compared with glioma cells suggest a tumor specific effect of this agent which is reflected in the cell cycle arrest seen in glioma cells but not NHA.

Effect on cyclin B1 levels and kinase activity of cyclin B1/cdk1 complex after vorinostat treatment

To determine if the removal of inhibitory phosphorylation of cdk1 that we observed resulted in increase activity of the cdk1/cyclin B1 complex, we examined the kinase activity of the complex using histone H1, a well-known substrate for the cdk1/cyclin B1 kinase activity. Vorinostat treated cells showed a reduction in phosphorylation of the histone H1 substrate suggesting a decrease in the kinase activity of cdk1/cyclin B1 (Fig. 5a). Given that cdk1 levels did not explain the G2 arrest seen, we assessed the levels of its binding partner, cyclin

B1. Treatment of glioma cells with increasing doses of vorinostat (0–10 μM) resulted in a decrease in the levels of cyclin B1 (Fig. 5b, upper panel). This effect was also seen in lower more clinically relevant doses of vorinostat (Fig. 5b lower panel, *note:* actin control for this blot is shared by p21 blot in Fig. 3c). Additionally, the decrease in cyclin B1 became more pronounced in a time-dependent manner (Fig. 5c). Pretreatment of cells with MG132, a proteosomal inhibitor, prior to drug treatment did not affect vorinostat-induced reduction of cyclin B1 levels ($P = 0.34$, NS) (Fig. 5d) suggesting that it was not proteosomally degraded. Analysis of levels of cyclin B1 transcript by qRTPCR in vorinostat treated cells showed a 5–15 fold reduction of cyclin B1 transcript level suggesting that cyclin B1 was reduced by transcriptional downregulation and not proteosomal protein degradation (Fig. 5e). These data suggest that vorinostat-induced decrease in cyclin B1 levels and increase in p21 levels are likely responsible for the G2 arrest seen.

Effect of vorinostat on organotypic human glioma cultures

Human tumor cell lines have limitations as a model because they accumulate genetic alterations during serial passaging that can dramatically alter their biological behavior. However, there are few mechanisms other than clinical trials that permit testing of the effects of new agents in viable human tissue. To address this shortcoming, we developed a novel organotypic human glioma slice culture model by modifying the hippocampal slice culture technique used in neurophysiologic studies. We utilized modifications in the buffers and culture media allowing us to maintain viable tumor slices for several days in culture; this provided us with a unique opportunity to test the effects of drugs on ex vivo human glioma tissue (Fig. 6a). Slice cultures, generated from freshly resected human glioblastoma (WHO grade IV) specimens, were exposed to vorinostat (3 μM) and subsequently assessed for changes in levels of p21 by immunoblotting. To ascertain whether the tissue remained over the period of the experiment, control glioma slices in each experiment were transduced with an adenovirus expressing enhanced green fluorescent protein (Ad-EGFP) and the fluorescence was monitored. Vorinostat-treated glioma slices derived from two patients with recurrent glioblastoma demonstrated an increase in p21 levels consistent with the expected class-effect of HDAC inhibitors (Fig. 6b). To confirm that characteristic effects of HDAC inhibition were achieved in human tumor tissue, glioma slices were treated with this agent and harvested at 5 and 24 h; these specimens demonstrated hyperacetylation of histones confirming that HDAC inhibition was achievable in these human tissue specimens upon direct exposure to vorinostat. To determine the effects of vorinostat on the other G2 checkpoint proteins, changes in levels of cyclin B1 and cdk1 levels were also assessed; levels of phospho-cdk1 in treated cells decreased rapidly by 1 h, remained low at 5 h and recovered to untreated levels whereas total cdk1 levels remained unchanged (Fig. 6c). Cyclin B1 levels showed a mild and transient decrease at 5 h but not at 1 or 24 h compared with untreated controls. The minimal nature of these changes may be related to the overall low proportion of cycling cells in tumor tissue. In a specimen with matched tumor and non-tumor specimens, vorinostat treated tumor slices demonstrated hyperacetylation of histone H3 and H4 (Fig. 6d). In comparison, non tumor brain tissue (obtained from superficial cortical tissue resected to access the tumor from the same patient) showed only a slight increase in acetylation of histone H3 and H4 upon exposure to vorinostat; this specimen consisted predominantly of nontumor tissue as verified by the pathologist. In addition, an increase in p21 levels similar to that seen in cell lines was seen in the tumor specimen but not in the non-tumor slices suggesting a differential effect for vorinostat in a tumor-specific manner. These results suggest that human glioma tissue when exposed to vorinostat exhibits characteristic changes induced by HDAC inhibition which appears to be tumor specific.

Discussion

Vorinostat induced a biologically relevant G2 cell cycle arrest in glioma cells related to an increase in p21 levels and reduced cyclin B1 and associated with a dose dependent decrease in anchorage-independent growth. The relative contribution of upregulation of p21 and reduction of cyclin B1 levels to the cell cycle arrest remains to be determined; however, given that either of these alterations would reduce cdk1 kinase activity, both changes likely contribute to induction of the cell cycle effects of vorinostat. The increase in p21 levels was independent of p53 activation; alteration of cyclin B1 was a result of transcriptional downregulation. NHA differed from the glioma cell lines in that no significant decrease was seen in cdk1 levels by 24 h; while a decrease in p-cdc25c was seen, total cdc25c levels remained without significant changes at 24 h. These findings may explain the lack of cell cycle effects in NHA at the same period as in the glioma cells.

Histone hyperacetylation and apoptosis were also seen in NHA raising the issue of potential toxicity to astrocytes in vivo. However, in a study using a mouse model with intact blood brain barrier, no neurotoxicity was seen after systemically administered vorinostat despite HDAC inhibition as demonstrated by hyperacetylation of brain tissue [17]. Additionally, in a recent clinical trial of vorinostat against recurrent glioblastoma (GBM) which showed evidence of antitumor activity [22], there was no evidence of neurotoxicity (E. Galanis, personal communication) suggesting that the data from in vitro studies using cultured NHA may not accurately reflect the in vivo normal tissue response in humans.

Direct demonstration of anti-tumor effects of an agent in human tumor tissue is challenging and usually requires clinical trials with correlative tissue studies. Activity of vorinostat in intracranial tumor models has been demonstrated in a human xenograft (U87 cells) and murine glioma models [23–25]; but, these have well recognized limitations and uncertain relevance to human gliomas. The ex vivo slice culture model that we utilized provides a new method of testing effects of therapeutic agents in viable human glioma tissue and clearly demonstrated the effects of vorinostat which was more strikingly seen in tumor tissue compared with non-tumor brain tissue from the same patient. The superficial cortical specimen used in our study as a non tumor control has limitations in that it is predominantly comprised of neurons which may not be representative of other types of normal brain cells. Also, brain tissue adjacent to tumor could potentially have infiltrative tumor cells which may influence the results. These effects need to be verified in more specimens to confirm our findings. Despite these limitations, the organotypic tumor slice culture system is a promising model for testing drug effects on human gliomas. To our knowledge, this is the first study to utilize organotypic slice cultures from viable human glioma tissues to test drug effects.

The development of epigenetically targeted treatments provides a novel strategy for both single agent and combination therapy approaches against malignant gliomas. As demonstrated in this study, the cellular effects of such agents need to be specifically delineated in each malignancy to provide a relevant context for strategic development of these agents in order to maximize their potential to provide a meaningful impact on patient prognosis.

Acknowledgments

This study was supported in part by funds from Brain Tumor SPORE 5P50CA12700102, The Gregory J. Jungeblut Fund for Brain Cancer Research, The Center for Targeted Therapy Grant and The Pennebaker Research Funds. The authors acknowledge Susan O. Graham, RN, Angele K. Saleeba, Kristin L. Parks, Lamonne Crutcher and Alicia A. Ledoux for their assistance with the study.

References

1. Holland EC. Gliomagenesis: genetic alterations and mouse models. Nat Rev. 2001; 2:120–129.
2. Penas-Prado M, Gilbert MR. Molecularly targeted therapies for malignant gliomas: advances and challenges. Expert Rev Anticancer Ther. 2007; 7:641–661. [PubMed: 17492929]
3. Baylin SB. DNA methylation and gene silencing in cancer. Nat Clin Pract. 2005; 2(Suppl 1):S4–S11.
4. Jones PA, Baylin SB. The epigenomics of cancer. Cell. 2007; 128:683–692. [PubMed: 17320506]
5. Amatya VJ, Naumann U, Weller M, Ohgaki H. TP53 promoter methylation in human gliomas. Acta Neuropathol. 2005; 110:178–184. [PubMed: 16025287]
6. Fukushima T, Katayama Y, Watanabe T, Yoshino A, Ogino A, Ohta T, Komine C. Promoter hypermethylation of mismatch repair gene hMLH1 predicts the clinical response of malignant astrocytomas to nitrosourea. Clin Cancer Res. 2005; 11:1539–1544. [PubMed: 15746058]
7. Hong C, Maunakea A, Jun P, Bollen AW, Hodgson JG, Gold-enberg DD, Weiss WA, Costello JF. Shared epigenetic mechanisms in human and mouse gliomas inactivate expression of the growth suppressor SLC5A8. Cancer Res. 2005; 65:3617–3623. [PubMed: 15867356]
8. Jiang Z, Li X, Hu J, Zhou W, Jiang Y, Li G, Lu D. Promoter hypermethylation-mediated down-regulation of LATS1 and LATS2 in human astrocytoma. Neurosci Res. 2006; 56:450–458. [PubMed: 17049657]
9. Richon VM, Emiliani S, Verdin E, Webb Y, Breslow R, Rifkind RA, Marks PA. A class of hybrid polar inducers of transformed cell differentiation inhibits histone deacetylases. Proc Natl Acad Sci USA. 1998; 95:3003–3007. [PubMed: 9501205]
10. Sawa H, Murakami H, Ohshima Y, Sugino T, Nakajyo T, Kisanuki T, Tamura Y, Satone A, Ide W, Hashimoto I, Ka-mada H. Histone deacetylase inhibitors such as sodium butyrate and trichostatin A induce apoptosis through an increase of the bcl-2-related protein Bad. Brain Tumor Pathol. 2001; 18:109–114. [PubMed: 11908866]
11. Wang ZM, Hu J, Zhou D, Xu ZY, Panasci LC, Chen ZP. Trichostatin A inhibits proliferation and induces expression of p21W AF and p27 in human brain tumor cell lines. Ai Zheng. 2002; 21:1100–1105. [PubMed: 12508652]
12. Arnold NB, Arkus N, Gunn J, Korc M. The histone deacetylase inhibitor suberoylanilide hydroxamic acid induces growth inhibition and enhances gemcitabine-induced cell death in pancreatic cancer. Clin Cancer Res. 2007; 13:18–26. [PubMed: 17200334]
13. Duvic M, Zhang C. Clinical and laboratory experience of vorinostat (suberoylanilide hydroxamic acid) in the treatment of cutaneous T-cell lymphoma. Br J Cancer. 2006; 95(Suppl 1):S13–S19.
14. Emanuele S, Lauricella M, Carlisi D, Vassallo B, D'Anneo A, Di Fazio P, Vento R, Tesoriere G. SAHA induces apoptosis in hepatoma cells and synergistically interacts with the proteasome inhibitor Bortezomib. Apoptosis. 2007; 12:1327–1338. [PubMed: 17351739]
15. Rosato RR, Almenara JA, Kolla SS, Maggio SC, Coe S, Gimenez MS, Dent P, Grant S. Mechanism and functional role of XIAP and Mcl-1 down-regulation in flavopiridol/vorinostat antileukemic interactions. Mol Cancer Ther. 2007; 6:692–702. [PubMed: 17308065]
16. O'Connor OA. Clinical experience with the novel histone deacetylase inhibitor vorinostat (suberoylanilide hydroxamic acid) in patients with relapsed lymphoma. Br J Cancer. 2006; 95(Suppl 1):S7–S12.
17. Hockly E, Richon VM, Woodman B, Smith DL, Zhou X, Rosa E, Sathasivam K, Ghazi-Noori S, Mahal A, Lowden PA, Steffan JS, Marsh JL, Thompson LM, Lewis CM, Marks PA, Bates GP. Suberoylanilide hydroxamic acid, a histone deacetylase inhibitor, ameliorates motor deficits in a mouse model of Huntington's disease. Proc Natl Acad Sci USA. 2003; 100:2041–2046. [PubMed: 12576549]
18. Puduvalli VK, Sampath D, Bruner JM, Nangia J, Xu R, Kyritsis AP. TRAIL-induced apoptosis in gliomas is enhanced by Akt-inhibition and is independent of JNK activation. Apoptosis. 2005; 10:233–243. [PubMed: 15711939]
19. Richon VM. Cancer biology: mechanism of antitumour action of vorinostat (suberoylanilide hydroxamic acid), a novel histone deacetylase inhibitor. Br J Cancer. 2006; 95(Suppl 1):S2–S6.

20. Arooz T, Yam CH, Siu WY, Lau A, Li KK, Poon RY. On the concentrations of cyclins and cyclin-dependent kinases in extracts of cultured human cells. Biochemistry. 2000; 39:9494–9501. [PubMed: 10924145]

21. Takizawa CG, Morgan DO. Control of mitosis by changes in the subcellular location of cyclin-B1-cdk1 and Cdc25C. Curr Opin Cell Biol. 2000; 12:658–665. [PubMed: 11063929]

22. Galanis E, Jaeckle KA, Maurer MJ, Reid JM, Ames MM, Hardwick JS, Reilly JF, Loboda A, Nebozhyn M, Fantin VR, Richon VM, Scheithauer B, Giannini C, Flynn PJ, Moore DF Jr, Zwiebel J, Buckner JC. Phase II trial of vorinostat in recurrent glioblastoma multiforme: a north central cancer treatment group study. J Clin Oncol. 2009; 27(12):2052–2058. [PubMed: 19307505]

23. Ugur HC, Ramakrishna N, Bello L, Menon LG, Kim SK, Black PM, Carroll RS. Continuous intracranial administration of suberoylanilide hydroxamic acid (SAHA) inhibits tumor growth in an orthotopic glioma model. J Neurooncol. 2007; 83:267–275. [PubMed: 17310267]

24. Yin D, Ong JM, Hu J, Desmond JC, Kawamata N, Konda BM, Black KL, Koeffler HP. Suberoylanilide hydroxamic acid, a histone deacetylase inhibitor: effects on gene expression and growth of glioma cells in vitro and in vivo. Clin Cancer Res. 2007; 13:1045–1052. [PubMed: 17289901]

25. Eyupoglu IY, Hahnen E, Buslei R, Siebzehnrubl FA, Savaskan NE, Luders M, Trankle C, Wick W, Weller M, Fahlbusch R, Blumcke I. Suberoylanilide hydroxamic acid (SAHA) has potent anti-glioma properties in vitro, ex vivo and in vivo. J Neurochem. 2005; 93:992–999. [PubMed: 15857402]

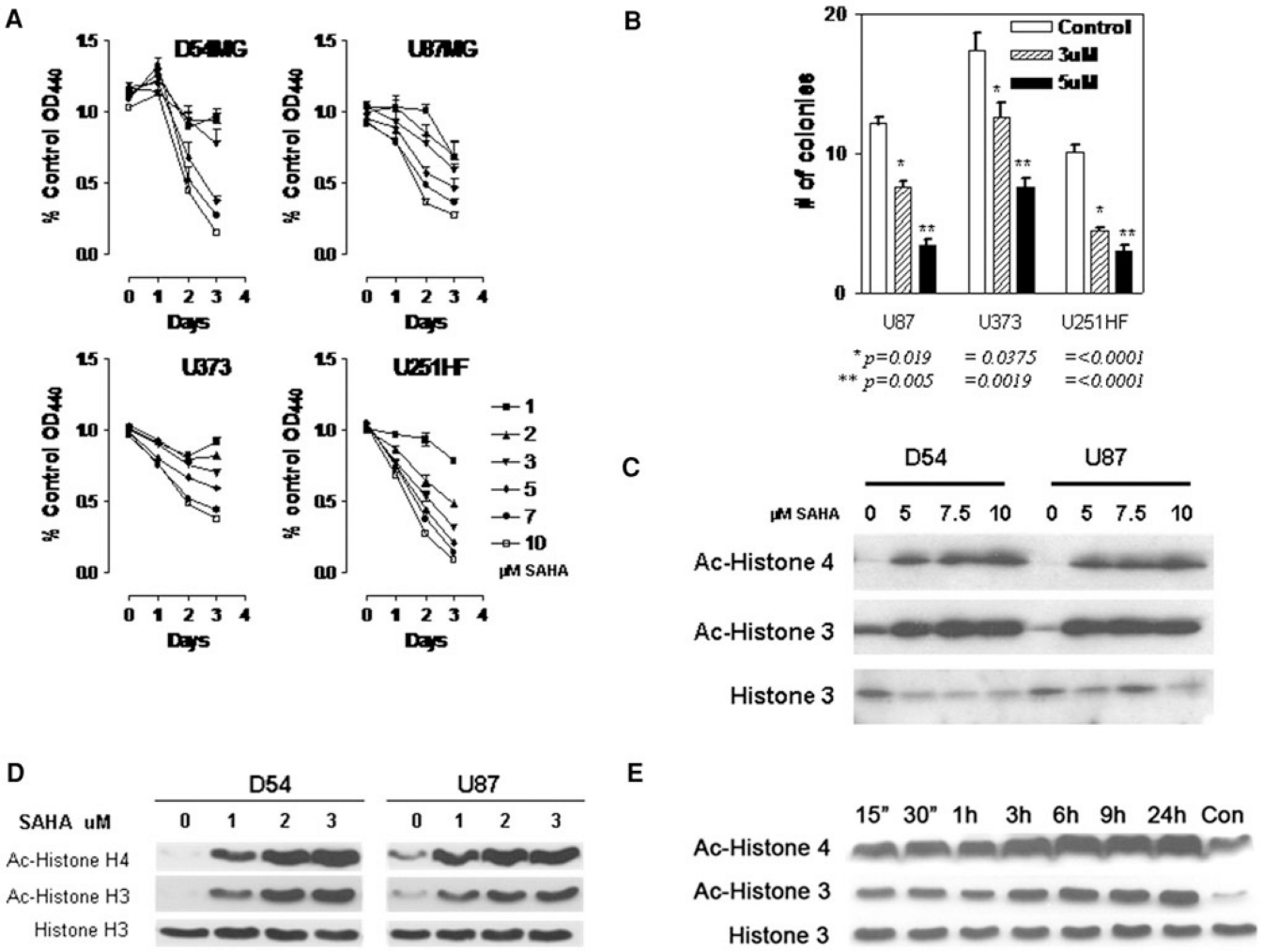

Fig. 1.

a Glioma cells were exposed to vorinostat at various concentrations as indicated and the proliferation rate assessed by change in colorimetric values using a WST-1 assay, **b** Cells were plated in soft agar at a density of 10 cells/well in six well plates and anchorage independent growth determined by determining nuMber of colonies formed. Data shown represent colony counts averaged from five high powered fields (error bars = standard error of mean; statistical analysis performed between control and treatment indicated using a unpaired *t*-test with a two-tailed *P* value with significant values being ≤0.05). **c** D54 and U87 glioma cells were treated with higher concentrations (5–10 μM) of vorinostat for 24 h and acetyla-tion of histones H3 and H4 were determined by immunoblotting. **d** Effect of lower concentrations (1–3 μM) of vorinostat on histone acetylation was assessed by immunoblotting. e Time course of histone acetylation after treatment of D54 cells with 3 μM vorinostat (untreated control at 24 h is shown in rightmost lane)

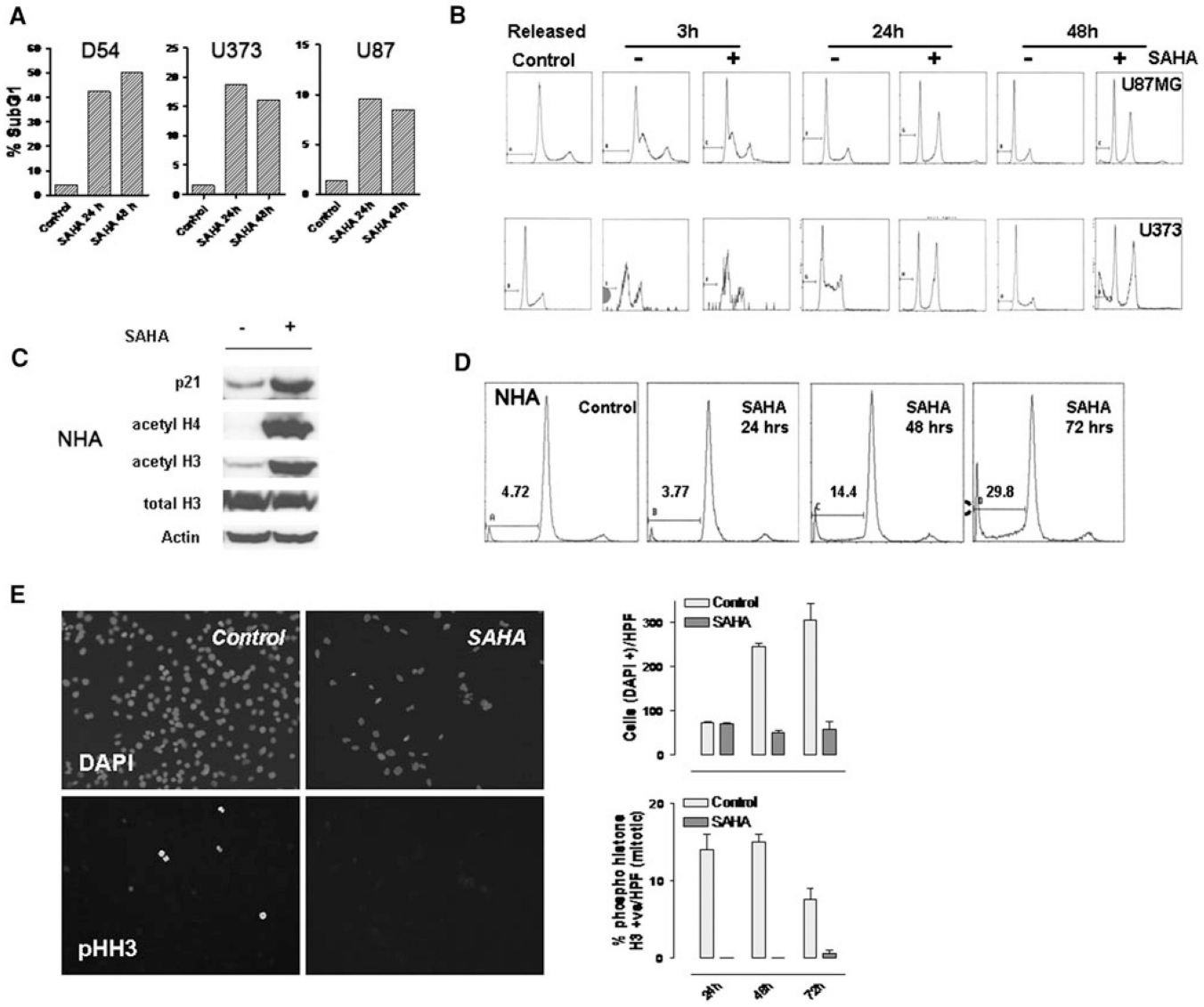

Fig. 2.

a D54, U373 and U87 cells were treated with vorinostat (3 μM) for 24 and 48 h and analyzed for apoptotic cells by flowcytometric measurement of the sub G1 cell cycle fraction. **b** Cells were synchronized in the G1 phase cell cycle boundary by a thymidine/urea double block, treated with vorinostat (3 μM) and released. Cells in each condition were harvested at the periods indicated and analyzed by flowcytometry. Data shown are representative of two independent experiments. **c** Normal huMan astrocytes (NHA) treated with vorinostat (3 μM) or vehicle (DMSO) were assessed for changes in p21 levels, acetylation of histones and total histone levels after 48 h of exposure to the agent. **d** NHA, cultured in astrocyte basal medium, were treated with vorinostat (3 μM); flowcytometric analysis was performed to detect cell cycle changes and the sub-G1 fraction at the times indicated. **e** D54 cells were cultured on coverslips and exposed to vorinostat (3 μM) for the periods indicated; the cells were fixed and immunostained with DAPI (to label nuclei) and phospho histone H3 (for mitotic cells). Mitotic and total cells were counted after appropriate immunostaining. Data shown in *graph* are the mean counts of positive cells derived from two independent measurements

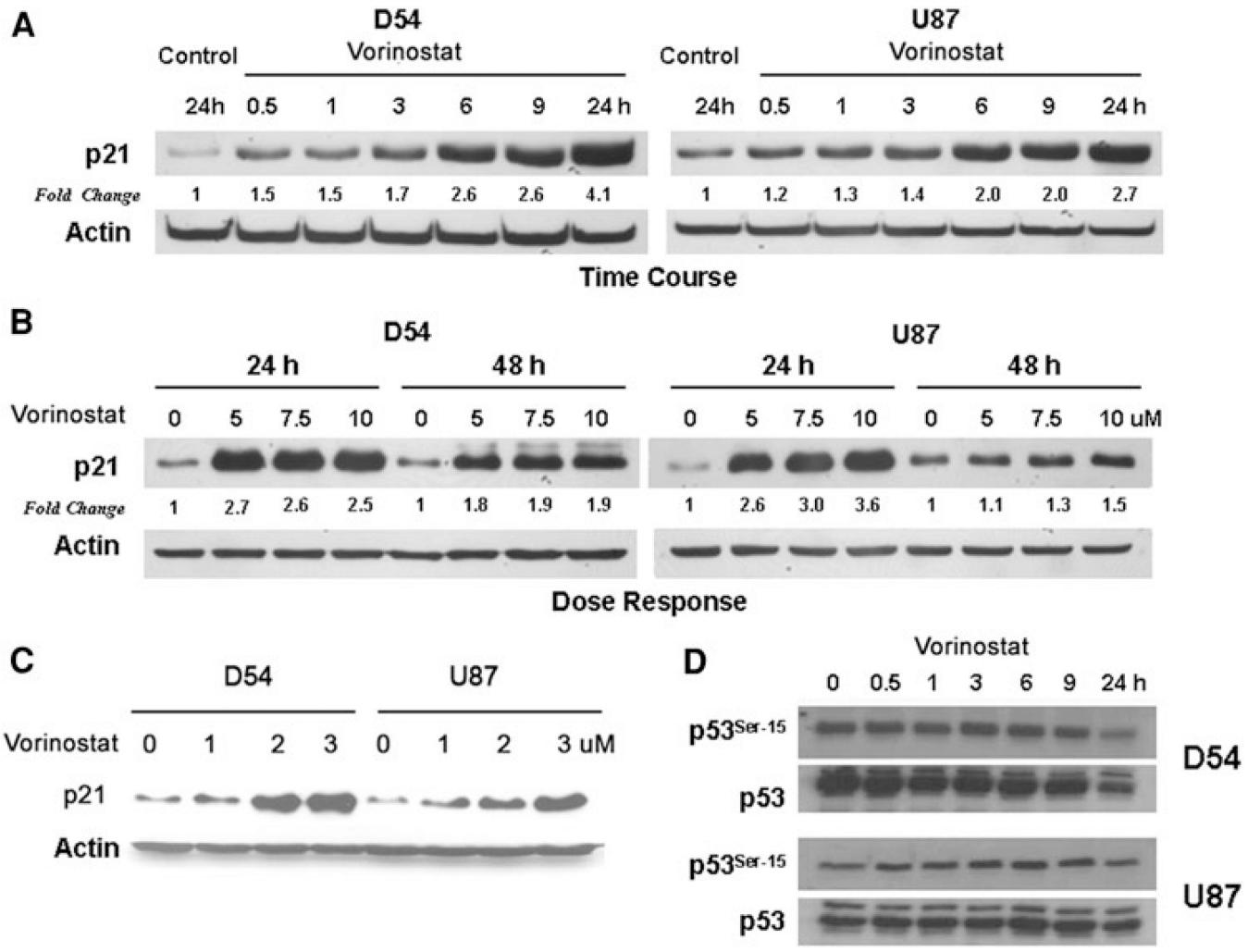

Fig. 3.

a D54 and U87 cells were exposed to vorinostat (3 μM) in a time-course experiment and harvested at the periods indicated. Levels of p21 were assessed by immunoblotting and actin levels were determined as a loading control. Fold change values (normalized to actin levels) compared to untreated control at 24 h are shown. **b** To determine the dose response relationship to vorinostat, cells were exposed to various higher concentrations (5–10 μM) of the agent and the levels of p21 determined by immunoblotting. **c** Changes in p21 levels were also assessed at lower concentrations (1–3 μM) of vorinostat with actin levels assessed as loading controls. **d** Phosphorylation status of p53 at Ser-15 was determined in comparison with total p53 levels at the periods indicated after exposure to vorinostat (3 μM)

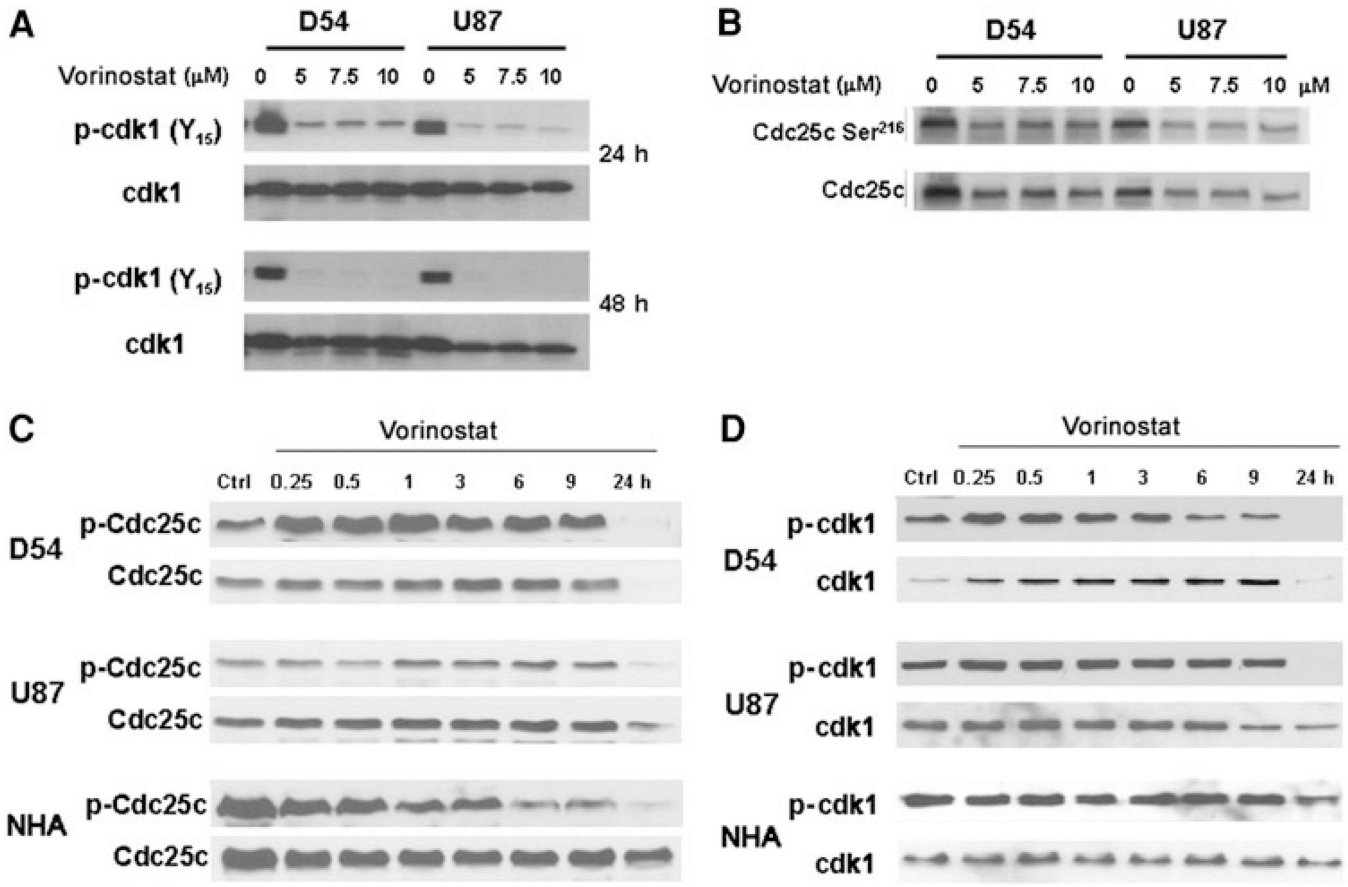

Fig. 4.

a Changes in level of inhibitory phosphorylation of cdk1 after treatment with vorinostat was determined at 24 and 48 h (using a Tyr-15 residue phospho-specific antibody) along with total cdk1 as loading control. **b** Degree of inhibitory phosphorylation of cdc-25 at Ser-216 was assessed by immunoblotting in response to increasing doses of vorinostat. **c** Time course of changes in phospho-cdc25c levels after exposure to vorinostat (5 μM). **d** Time course of changes in levels of phospho-cdk1 and total cdk-1 were determined following treatment with vorinostat (5 μM)

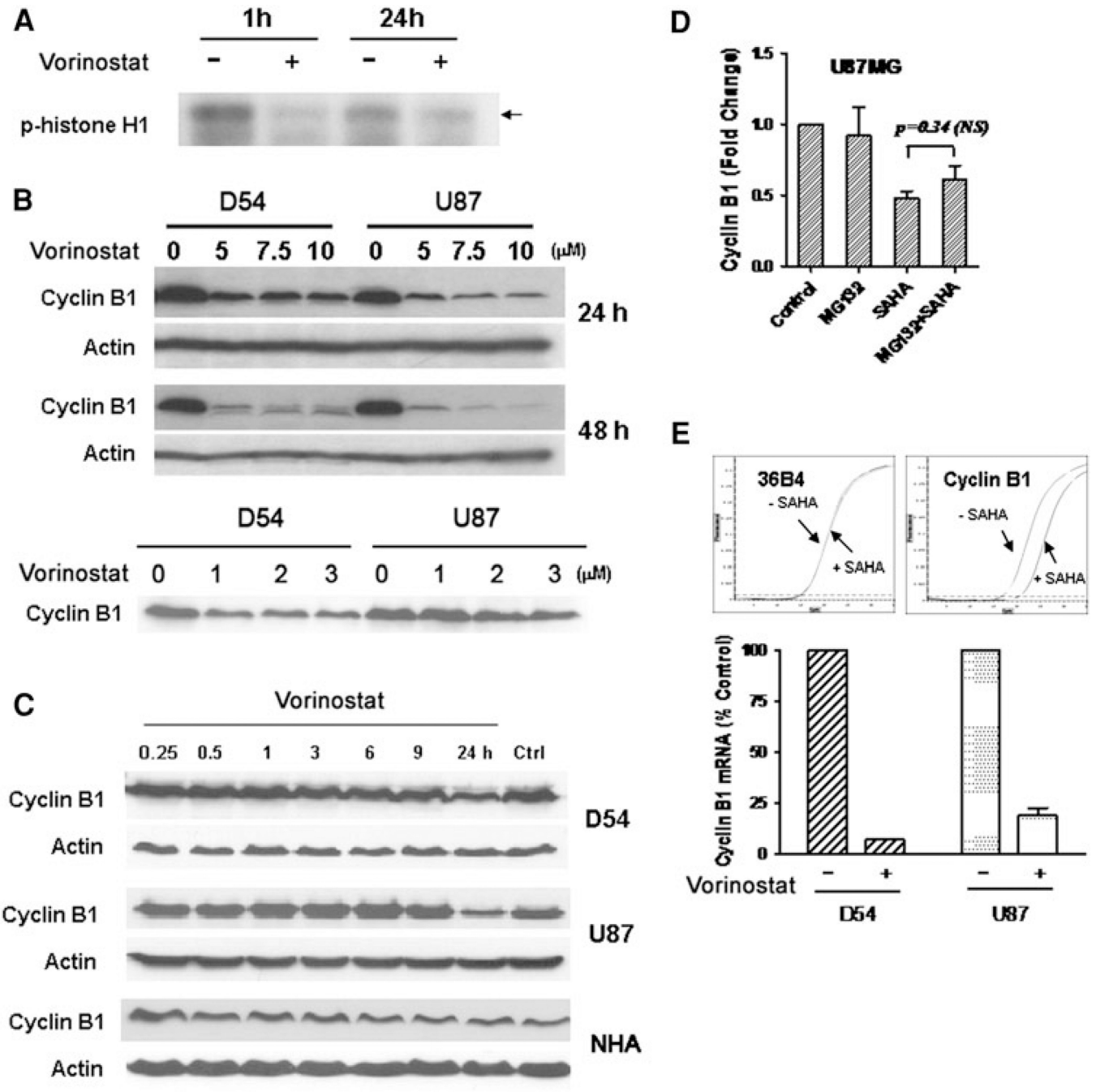

Fig. 5.

a Cells treated with vorinostat (3 μM) for the periods indicated were assessed for kinase activity of the cdk1/cyclin B1 complex in an in vitro kinase assay using histone H1 as a substrate. The cell lysates were subsequently subject to immunoblotting using an anti phospho-histone H1 antibody, **b** Cyclin B1 levels were determined in D54 and U87 cells after treatment with various doses of vorinostat at 24 and 48 h (higher concentrations, *upper panel*; lower concentrations, *lower panel*) (*note* the actin control for the upper panel blot is shared by that for the p21 in Fig. 3c). **c** D54, U87 and NHA cells were treated with vorinostat (3 μM) and the time course of changes in cyclin B1 levels were assessed by immunoblotting. **d** U87MG cells were treated with vorinostat alone (3 μM), MG132 alone,

or MG132 followed by vorinostat. Levels of cyclin B1 were determined by immunoblotting and the intensity of the bands were quantitated and expressed relative to levels in untreated control. Statistical analysis was performed between vorinostat alone or vorinostat plus MG132 using a unpaired *t*-test with a two-tailed *P* value; significant values are ≤ 0.05). **e** Levels of cyclin B1 transcript in D54 and U87 cells were determined by quantitative real-time PCR (*upper panel*) after treatment with vorinostat (3 μM) and with transcript levels of the ribosomal protein 36B4 as a control. Mean C_T levels of cyclin B1 transcript (*lower panel*) are shown relative to levels of 36B4 transcript

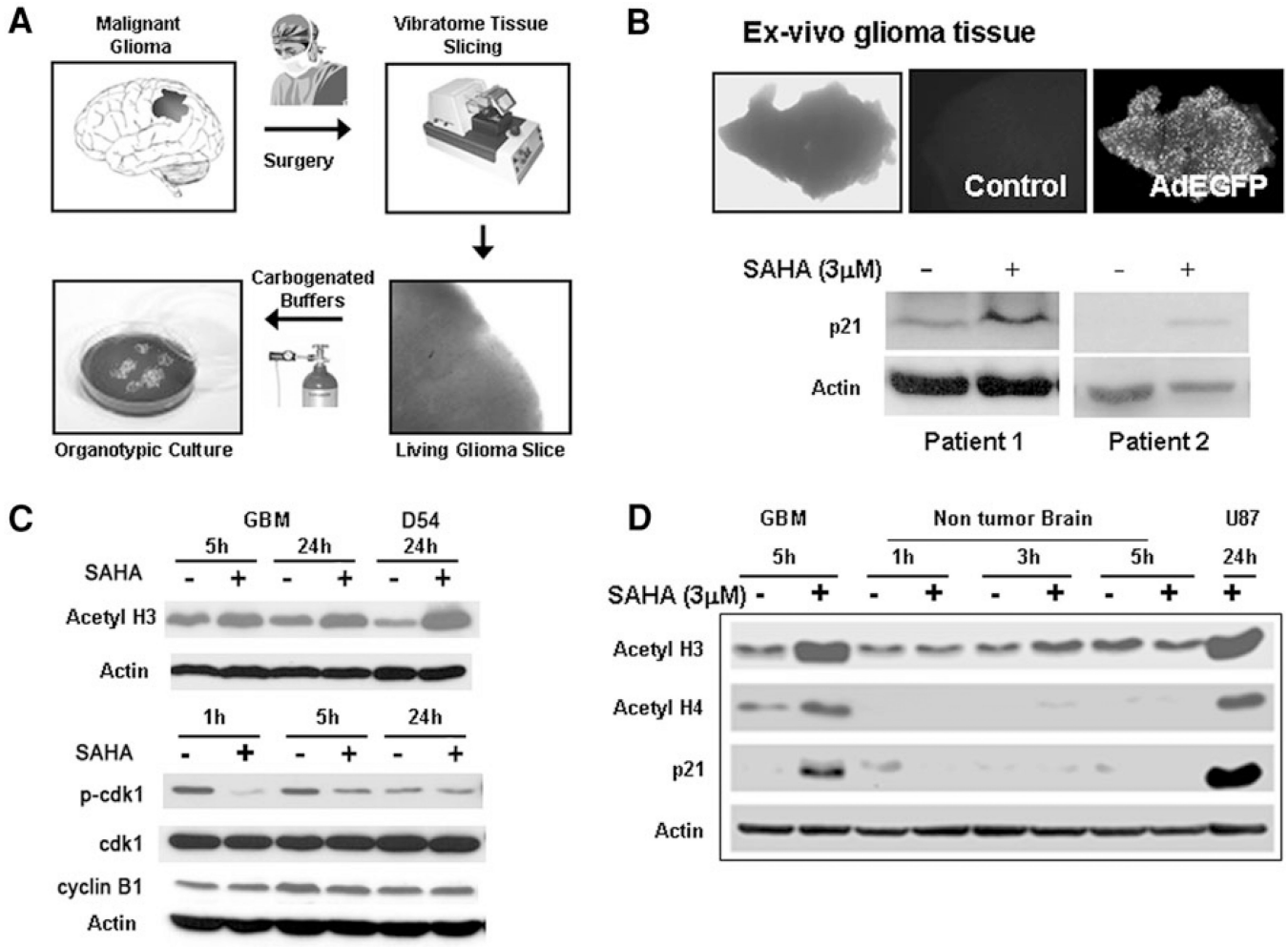

Fig. 6.

a Generation of organotypic human glioma tissue slices: freshly resected tumor tissue was obtained from patients undergoing surgical removal of malignant gliomas and 300 urn thick slices were generated using a Vibratome. The slices were maintained in carbogenated ACSF and subsequently incubated at 37°C. **b** Tissue slices derived from freshly resected human glioblastoma specimens were incubated with vorinostat or vehicle control for 48 h and subsequently homogenized to generate protein lysates. Levels of p21 were determined by immunoblotting. Viability of the slices during the course of the experiment was assessed by simultaneously monitoring fluorescence signal from control slices transduced with an adenoviral construct expressing EGFP. **c** Glioma slices were treated with vorinostat (3 μM) or PBS for the periods indicated and the levels of histone acetylation, phospho-cdk1 and total cdk1, and cyclin B1 were determined by western blots. Actin levels were obtained as a loading control. **d** Tissue slices generated from a human glioblastoma specimen and from overlying non-tumor cortical brain tissue were treated with vorinostat (3 μM) and levels of acetyl histones and p21 determined in the lysates derived from the slice homogenates. Lysates from U87 cells treated with vorinostat (3 μM) were used as a control. Actin levels were determined both as a loading control and to determine the integrity of proteins in the tissue slices